JOURNAL OF CATALYSIS 58, 419–435 (1979)

Physicochemical Properties of MnO_2 and MnO_2–CuO and Their Relationship with the Catalytic Activity for H_2O_2 Decomposition and CO Oxidation

SUKRITI B. KANUNGO

Regional Research Laboratory, Bhubaneswar—751013, Orissa, India

Received January 16, 1978; revised September 28, 1978

The catalytic activity of MnO_2 prepared by different methods has been determined from the initial rate of decomposition of H_2O_2 and the conversion of CO to CO_2. The activity is correlated with various physicochemical properties such as active oxygen, surface excess oxygen, surface OH groups, crystalline modifications, lattice parameters, and thermal decomposition data. Some of the above properties are interrelated. Experimental evidence shows that the presence of Mn^{3+} as MnOOH in the MnO_2 lattice is mainly responsible for the origin of catalytic activity in nonstoichiometric manganese dioxide where electron transfer between Mn^{4+} and Mn^{3+} ions can take place. The loss of strongly bound compositional water creates lattice defects which are also responsible for the increase in the catalytic activity. The reason for the promoting effect of CuO in MnO_2–CuO catalysts has been discussed in the light of the formation of "surface $CuMn_2O_4$" through the exchange of Cu^{2+} on the hydrated manganese oxide surface.

INTRODUCTION

The high activity of manganese dioxide for the catalytic oxidation of CO and the decomposition of H_2O_2 is well known. Not only manganese dioxide but also some nonstoichiometric higher oxides of manganese having the formular MnO_x (where $2 > x > 1.5$) are active catalysts (*1*, *2*). The activity of such manganese oxide catalysts is promoted (*3*) by admixing other oxides such as CuO, NiO, Co_2O_3, or Ag_2O. It is well known that nonstoichiometric oxides of manganese exist in various crystalline polymorphic forms and that their physicochemical characteristics sometimes vary widely depending upon the method of preparation. It has been observed (*4*) that only a few crystalline modifications of MnO_2 show satisfactory activity as depolarizers in the Leclanché cells. Attempts were made to find out if such preferential activity exists toward various catalytic oxidation reactions. Thus Ball *et al.* (*5*) and Turner (*6*) were unable to oxidize benzyl alcohol over MnO_2 prepared by one method, whereas Harfeinst *et al.* (*7*) and Highet and Wildman (*8*) obtained benzaldehyde in excellent yield under the same conditions using MnO_2 obtained by a different method of preparation. A literature survey reveals that since the early investigation by Pitzer and Frazer (*9*) little attention has been given to the study of the catalytic behavior of MnO_2 prepared by different methods especially in the presence of CuO and its relationship with various surface and other properties of the catalysts. The object of this paper is to report and explain some results toward this end.

0021-9517/79/090419-17$02.00/0

EXPERIMENTAL METHODS

Preparation of the Catalysts

All the reagents used in the present investigation were of analytical grade (E. Merck, G.R.). All the manganese oxide (MnO_x) catalysts prepared by the following methods were thoroughly washed with water until free from adhering ions and then dried at 110 to 120°C for 6 to 8 hr. Unless otherwise stated, the two component catalyst system (MnO_x–CuO) was prepared by precipitating $Cu(OH)_2$ in the presence of MnO_x catalysts by adding 1:3 NH_4OH to Cu(II) nitrate solution till the final pH was 6.5 to 7.0. The precipitates after thorough washing was first dried at 110 to 120°C and then calcined at 200°C for 4 hr. The ratio of MnO_x to CuO in the dried product was about 60:40. For the determination of catalytic activity toward the oxidation of CO all the catalyst samples were further calcined at 300°C for 2 hr. The following catalyst samples were used in the present work.

Sample 1. Oxidation of Mn(II) nitrate with $KMnO_4$ at the boiling point until the supernatant liquid shows slightly pink color.

Sample 2. Prepared by the method of Pitzer and Frazer (*2*) by adding $KMnO_4$ to an aqueous solution containing Mn(II) and Cu(II) nitrates in the molar ratio of 3:2.

Sample 3. Same as in method 2 except that the salt solution was added to the $KMnO_4$ solution.

Sample 4. $Cu(OH)_2$ was precipitated in the presence of sample 3.

Sample 5. Reduction of $KMnO_4$ solution at 70 to 80°C with 1:1(v/v) HCl.

Sample 6. Sample 5 was leached in 3 *M* HNO_3 at 90°C for about 120 min.

Sample 7. $Cu(OH)_2$ was precipitated in the presence of sample 6.

Sample 8. Oxidation of $MnSO_4$ in hot acidified (2 *N* H_2SO_4) solution by ammonium persulfate.

Sample 9. $Cu(OH)_2$ was precipitated in the presence of sample 8.

Sample 10. Thermal decomposition of Mn(II) nitrate at 130 to 150°C for about 8 hr and finally grinding to less than 150 μm.

Sample 11. Simultaneous thermal decomposition of Mn(II) and Cu(II) nitrates at 130 to 150°C for 8 hr and grinding to <150 μm.

Sample 12. Oxidation of Mn(II) nitrate by sodium chlorate in strong nitric acid medium according to the method of Brooks (*10*).

Sample 13. $Cu(OH)_2$ was precipitated in the presence of sample 12.

Active Oxygen

Active (or available) oxygen was determined by the oxalate method. Manganese was estimated by the EDTA method in the presence of hydroxylammonium chloride and triethanolamine at pH 10. From these two values x in MnO_x was calculated.

Trivalent (Mn^{3+}) manganese was estimated from the stoichiometry of the following equation:

$$MnO + MnO_2 = Mn_2O_3.$$

Surface Oxygen

Two different methods of determination of surface oxygen based on the work of Uchijima *et al.* (*11*) were used. They are (i) by hydrazine reduction and (ii) with KI at pH 7.1. Whereas the hydrazine method is usually carried out at the pH (8.0–8.5) of 0.1 *N* hydrazine sulfate solution, the KI method is highly dependent upon the pH of the medium. However, for the sake of comparison of the different catalyst samples the KI method was carried out in the presence of phosphate buffer (pH 7.1).

In method (i) a measured amount of 0.1 *N* hydrazine sulfate solution is allowed to react with a known weight of catalyst

sample for about 20 to 25 min in a closed vessel. The residual hydrazine after filtration was titrated against 0.1 *N* iodine solution at pH 7.2.

In method (ii) a known amount of catalyst sample, 15 ml of buffer solution, and about 2 g of solid KI were placed in a closed vessel which was vigorously shaken for 7 hr. The reaction mixture was then filtered, washed with methanol, and acidified with 1 *N* HCl, and the liberated iodine was titrated against 0.01 *N* sodium thiosulfate using starch as indicator.

Surface OH Groups

The method was developed by Laragne and Brenet (*12*) for the determination of surface OH groups in MnO_2. A known weight of catalyst sample (0.05 g) together with 20 ml of dimethylformamide (DMF) and about 2 g of KI were shaken thoroughly in a stoppered vessel for about 4 hr. The reaction mixture was then filtered and washed with DMF, and the liberated iodine was titrated against 0.01 *N* thiosulfate solution without an indicator.

X-Ray and Thermal Analysis

X-Ray powder diffraction photographs were taken using Fe$K\alpha$ radiation with a manganese filter for MnO_2 samples and Cu$K\alpha$ radiation with a Ni filter for MnO_2–CuO catalysts. Various crystalline modifications of MnO_2 were identified with the help of ASTM cards.

Thermal analysis was carried out using a MOM (Budapest, Hungary) Derivatograph at a heating rate of 10°C/min. DTA, DTG, and TG sensitivities were $\frac{1}{10}$, $\frac{1}{10}$, and 200 mg, respectively. The sample weight varied from 300 to 800 mg depending upon the bulk density of the sample.

Surface Areas

Surface areas of the catalyst samples were determined with a high speed surface area analyzer (Micromeritics Instruments Corporation) Model No. 2200, using low-temperature (−196°C) nitrogen adsorption.

Test for Catalytic Activity

Decomposition of H_2O_2. The decomposition of H_2O_2 was followed by measuring the volume of oxygen liberated at atmospheric pressure in a gas burette. All the experiments were carried out using 0.02 to 0.05 g catalyst and a 0.018 *M* solution of stabilizer-free H_2O_2. The total volume of oxygen that could be theoretically liberated was calculated from the known concentration of H_2O_2 and finally corrected for room temperature and pressure. Rate of decomposition was determined at five different temperatures in the range of 20 to 40°C.

Both first-order and second-order rate constants were determined. The second-order rate constant was determined by converting the volume of oxygen liberated to the concentration of H_2O_2 using the following formula (*13*):

$$C = C_0 - \frac{PV_g}{RTV_l}$$

where

C = concn of H_2O_2 at time t (moles liter^{-1})
C_0 = initial concn of H_2O_2 (moles liter^{-1})
P = atmospheric pressure ($\simeq$1 atm)
V_g = volume of oxygen liberated at time t (ml)
V_l = total volume of solution (ml).

Oxidation of CO. Oxidation of CO was carried out by passing a gas mixture containing 5% CO in air (v/v) at a flow rate of 21 ml/min successively through SiO_2 gel, fused $CaCl_2$, KOH pellets, and then through a 1-g catalyst bed packed in a tubular reactor immersed in a thermostat bath. The gas leaving the reactor was allowed to bubble through a known amount of $Ba(OH)_2$ solution containing one or two drops of phenolphthalein indicator. The

TABLE 1A

Kinetic Parameters of the Catalytic Decomposition of H_2O_2 and the Oxidation of CO over MnO_2 Catalyst Samples

Sample numbers	Decomposition of H_2O_2					Oxidation of CO	
	Order of reaction	Second-order rate constant (g^{-1} sec^{-1} $mole^{-1}$)	First-order rate constant (g^{-1} sec^{-1})	Initial rate of decomposition (30°C) (ml O_2 g^{-1} sec^{-1})	Ea (kcal $mole^{-1}$)	Ea (kcal $mole^{-1}$)	Conversion at 80°C (%)
1	2	5.425	—	1.114	14.29	—	—
2	2	7.347	—	1.213	15.18	—	—
3	2	3.605	—	1.650	9.39	5.53	45.0
5	1	—	0.1152	1.583	9.58	8.21	8.5
6	1	—	0.1008	1.237	4.83	13.86	12.5
8	Fractional (nearly 1.5)	—	0.0800	1.166	8.36	14.59	4.3
10	1	—	0.0200	0.200	—	9.12	3.8
12	1	—	0.0300	0.350	11.56	13.22	22.6

TABLE 1B

Kinetic Parameters of the Catalytic Decomposition of H_2O_2 and the Oxidation of CO over MnO_2–CuO Mixed Catalyst System

Sample numbers	Decomposition of H_2O_2			Oxidation of CO		
	First-order rate constant (sec^{-1} g^{-1} catalyst)	First-order rate constant (sec^{-1} g^{-1} MnO_2)	Ea (kcal/mole)	Conversion (%) at 40°C	Conversion (%) at 80°C	Ea (kcal/mole)
4	0.0441	0.0736	3.33	17.1	45.5	8.06
7	0.0384	0.0640	13.00	5.5	28.8	12.8
9	—	—	—	10.7	36.0	13.22
11	0.0250	0.0420	17.95	10.8	35.3	12.31
13	0.0320	0.0510	9.50	17.9	51.8	12.8

reciprocal of the time taken from the entrance of the first gas bubble into the solution to the disappearance of pink color gives the rate of oxidation of CO. The extent of conversion was calculated from the CO_2 required to neutralize a known amount of $Ba(OH)_2$. All the measurements were carried out under the steady-state conditions which was attained after 5 to 6 hr of continuous flow of gas mixture through the catalyst bed. Apparent activation energy values were obtained from the plots of log (percentage conversion) versus reciprocal of absolute temperature.

RESULTS

Kinetic Data for the Decomposition of H_2O_2

The decomposition of H_2O_2 on catalyst samples 1, 2, and 3 follows second-order kinetics up to 40°C, whereas the other MnO_2 catalysts follow almost first order with a break after about 40 to 50% decomposition. Incorporation of CuO by precipitating $Cu(OH)_2$ in the presence of MnO_2 catalysts does not promote the catalytic decomposition of H_2O_2 to an appreciable extent per gram of mixture; only a marginal increase is observed when

the rate constant is expressed per gram of MnO_2. Therefore, as far as the catalytic decomposition of H_2O_2 is concerned the present method of preparing the two-component (MnO_2–CuO) hopcalite system is not very useful. However, the presence of CuO causes the reaction to follow first-order kinetics, even for those samples which follow second order such as samples 1 to 3. Since the catalyst samples prepared by different methods exhibit different orders toward the decomposition of H_2O_2 and at the same time show a strong apparent compensation effect, the catalytic activities were compared by the initial rates of decomposition in terms of volume of oxygen liberated per second per gram of catalyst at 30°C. Results are shown in Tables 1A and 1B.

From the present experimental data it is difficult to explain the observed change in kinetic law (as well as activation energy) as the mechanism of the decomposition of H_2O_2 on metal oxides is a rather complicated one. However, on the basis of our existing knowledge of catalytic decomposition of H_2O_2 we may write the following reaction steps:

$$\text{(I)} \qquad H_2O_2 \rightleftharpoons H^+ + HO_2^-$$

$$\text{(II)} \qquad S^* + HO_2^- \rightleftharpoons (SO_2H)_{ads}$$

$$\text{(III)} \qquad (SO_2H)_{ads} + H_2O_2 \rightarrow H_2O + O_2 + OH^- + S^*$$

$$\text{(IV)} \qquad H^+ + OH^- \rightleftharpoons H_2O$$

where S* in step (II) is an Mn^{4+} site. Assuming that step (III) is rate controlling, the rate of decomposition will follow first order if the concentration (or number) of $(SO_2H)_{ads}$ is large in comparison with the concentration of H_2O_2, i.e., when the surface is extensively covered with HO_2^- ion. If this is not so (due to some unexplained reasons) the rate will be proportional to the concentrations of both H_2O_2 and HO_2^- which in turn is proportional to H_2O_2 concentration. Therefore, the reaction will follow second order. Perhaps the large amount of acidic OH groups in some samples is responsible for the low adsorption of HO_2^- ion on the catalyst surface.

Kinetic Data for the Oxidation of CO

Except for sample 3 the activity of all the manganese oxide catalysts used in the present work is poor for the low-temperature oxidation. The good activity of sample 3 is probably due to the adsorption of Cu^{2+} ions on the surface of MnO_x during its preparation. However, a considerable increase is recorded when CuO is introduced either by precipitation as $Cu(OH)_2$ or by simultaneous thermal decomposition of nitrates and subsequent calcination at 300°C. All the two component catalysts exhibit breaks in the Arrhenius plots at 50 to 60°C, so that an activity parameter could be obtained only at temperatures below 50°C, e.g., at 40°C where the reaction is predominantly chemically controlled. In comparison with the sharp increase in activity for such MnO_2–CuO catalysts there is only a marginal decrease in apparent activation energy. For single component catalysts the Arrhenius plots follow linear behavior up to 90°C and since at 40°C the conversions are very small activities are compared at 80°C. Results are shown in Tables 1A and 1B.

Physicochemical Characteristics

X-ray diffraction pattern. The brownish-colored dioxides such as sample 2, 3, 5, and 6 are partially amorphous in nature as revealed from the broad and diffuse diffraction patterns, whereas the black oxides are well crystallized as indicated by the sharp powder patterns of the samples. The powder patterns also show that all the four important polymorphic forms of MnO_2, viz. α, β, γ, and δ are present among the catalyst samples. However, some of them are admixtures of two

TABLE 2

Microstructural and Surface Properties of Manganese Dioxide Catalyst Samples

Sample numbers	x in MnO_x	Crystalline modification	Crystal system	Unit cell parameters			Surface area ($m^2\ g^{-1}$)	Surface oxygen atom/$cm^2 \times 10^{-14}$	
				a (Å)	b (Å)	c (Å)		Calculated from unit cell parameters	Obtained from KI (pH 7.1) method
1	1.989	γ	Orthorhombic	4.319	10.531	2.907	80.5	15.40	5.1
2	1.971	γ	—	—	—	—	81.0	—	5.6
3	1.948	γ(poorly crystalline)	Orthorhombic	4.338	8.906	2.881	71.2	17.31	12.3
5	1.915	δ	Hexagonal	5.815	5.815	13.060	85.0	16.69	10.1
6	1.886	α(with minor γ)	Pseudotetragonal	9.928	9.928	2.841	65.5	14.86	9.1
8	1.916	α	Tetragonal	9.928	9.928	2.851	31.0	14.84	14.1
10	1.992	β	Tetragonal	4.390	4.390	2.860	2.6	17.43	7.3
12	1.990	γ (or, ρ)	Orthorhombic	4.390	9.687	2.872	9.1	16.26	71.5

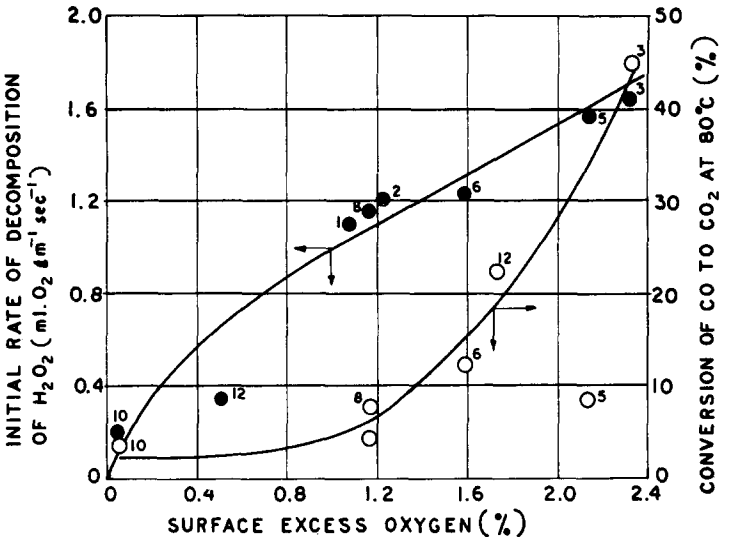

FIG. 1. Relationship between the surface excess oxygen determined by the KI (pH 7.1) method and the catalytic activity of the MnO_2 samples. Superscripts denote the catalyst sample numbers. ●, Initial rate of decomposition of H_2O_2 at 30°C; ○, conversion of CO to CO_2.

or more varieties. The indexing of the diffraction lines was carried out using an analytical method on the basis of some assumed symmetry which was verified from the similarity in the calculated and the observed d(Å) values. The unit cell parameters of the various MnO_2 catalyst samples are shown in Table 2. Diffraction patterns of sample 11 and 13 indicate the minor formation of surface compound such as $CuMn_2O_4$ in addition to the strongly predominant CuO lines (Fig. 9).

Surface and active oxygen content. The importance of both surface and active (or available) oxygen content of MnO_2 in the catalytic oxidation of CO has been emphasized by various authors (*14*, *15*). While the surface oxygen is essentially a surface property of the catalyst, active oxygen is a bulk property and therefore may not be wholly responsible for the catalytic oxidation reaction. However, the two different methods of estimating surface oxygen give different values, i.e., the results obtained by the hydrazine method is four to seven times higher than that determined by the KI (pH 7.1) method. Kobayashi *et al.* (*14*) also observed that the hydrazine method gives 15 to 25 times higher values than the KI (pH 7.1) method. This is probably because hydrazine attacks the bulk oxygen of the catalyst and reduces the MnO_2 while KI at pH 7.1 or above does not attack bulk oxygen to any appreciable extent. This is evident from the similarity in the order of magnitude of the surface oxygen content calculated from the unit cell parameters [0.67 power of the bulk concentration, Ref. (*10*)] and from the KI method as shown in Table 2. A high value for sample 12 indicates that a considerable amount of oxygen is chemisorbed on the surface.

Figures 1 and 2 show that the effect of surface oxygen content determined by both hydrazine and KI (pH 7.1) methods on the activity of MnO_2 catalysts. The nature of the effect of surface excess oxygen on the two catalytic reactions appears to be different. Although a higher surface oxygen content has a profound effect on the activity for the oxidation of CO, the same is not true for the decomposition of H_2O_2. On the other hand,

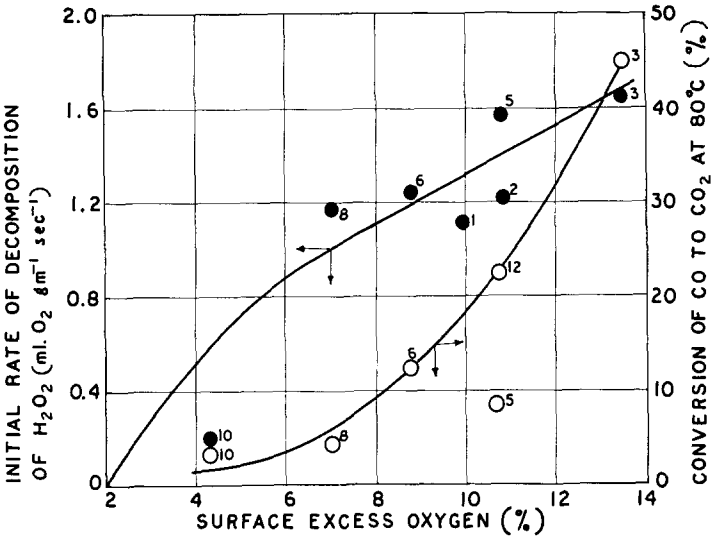

FIG. 2. Relationship between the surface excess oxygen determined by hydrazine method and the catalytic activity of the MnO_2 samples. Superscripts denote the catalyst sample numbers. ●, Initial rate of decomposition of H_2O_2 at 30°C; ○, conversion of CO to CO_2.

at a lower surface excess content its effect on the initial rate of decomposition of H_2O_2 is more pronounced than on the conversion of CO.

Surface OH groups. The effect of the presence of surface OH groups on the catalytic activity of MnO_2 can only be tested with the decomposition of H_2O_2 which is carried out in an aqueous medium since it is believed that the presence of water poisons the activity toward the oxidation of CO. In Fig. 3 the initial rate of decomposition of H_2O_2 at 30°C is plotted against the surface OH groups. The figure reveals that the rate of reaction increases logarithmically with increase in

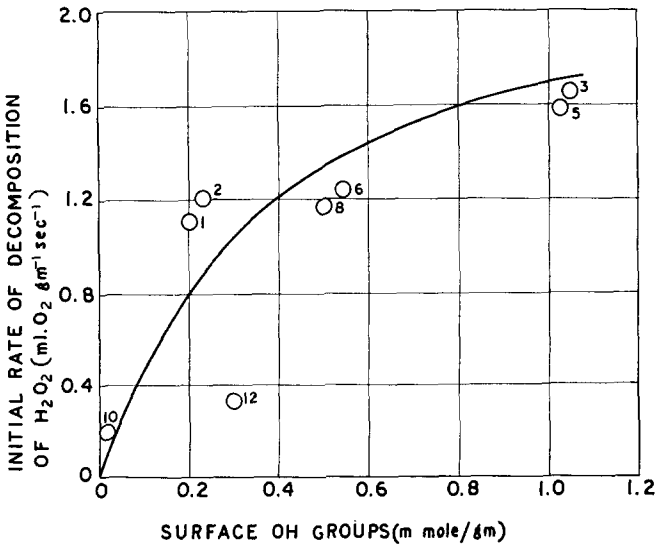

FIG. 3. Correlation between surface OH groups and the initial rate of decomposition of H_2O_2. Superscripts denote the catalyst sample numbers.

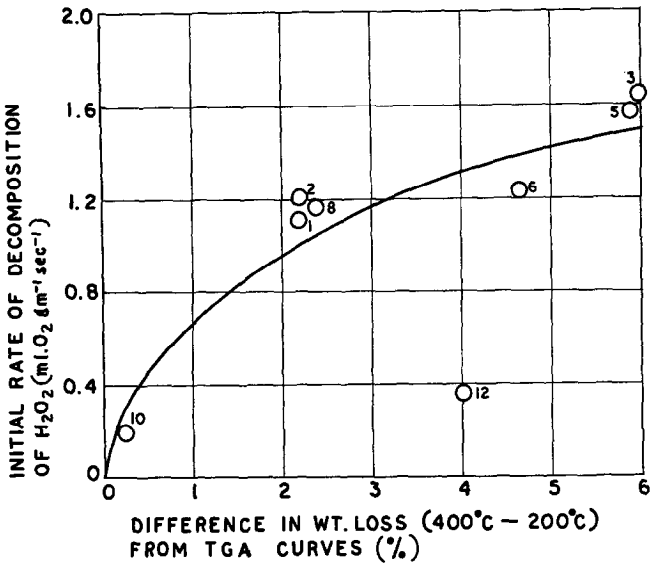

FIG. 4. Correlation between the difference in weight loss at 400 and 200°C (obtained from the TGA curves) and the initial rate of decomposition of H_2O_2. Superscripts denote the catalyst sample numbers.

OH groups indicating that a large quantity of OH groups does not help in increasing the activity of the catalyst. The interesting aspect of the method is that physically adsorbed water molecules do not take part in the exchange of H^+ (in OH group) with K^+ in DMF medium. Since at 200°C drying temperature all the physically adsorbed water molecules are lost and at 400°C both physisorbed and chemisorbed water are removed the difference in the weight loss at the two temperatures should give at least an order of magnitude of the amount of chemically bound water since nonstoichiometric MnO_2 may lose some oxygen with increase in calcination temperature. However, the amount of such oxygen loss at 400°C is very small as shown by Hasegawa *et al.* (*15*). Figure 4 shows that the relationship between the activity and the difference in weight loss at 400 and 200°C is very similar to that obtained in Fig. 3. The reason for the sharp deviation with sample 12 is probably the loss of some oxygen at 400°C.

Thermal analysis. Thermal analysis (25–1000°C) of MnO_2 catalysts prepared by various methods exhibits under dynamic conditions (i.e., with increasing temperature at constant heating rate) mainly four different thermal effects (Fig. 5). These are: (i) Loss of physically adsorbed molecular water (100–200°C) characterized by a sharp endothermic DTA and DTG peak accompanied by a well-defined stage in the TGA curve. (ii) Loss of chemically bound or compositional water and change of crystalline phase (for example, γ-MnO_2 to β-MnO_2) characterized by a broad exothermic hump which sometimes suppresses the endothermic effect due to the loss of compositional water in the temperature region of 200 to 400°C. Except for samples 1 and 12 the DTG peak in this temperature region is normally poorly defined. However, from the TG curve one can easily identify the second stage of water loss. (iii) Sharp endothermic effect for the decomposition of MnO_2 to Mn_2O_3 in the temperature range of 500 to 700°C

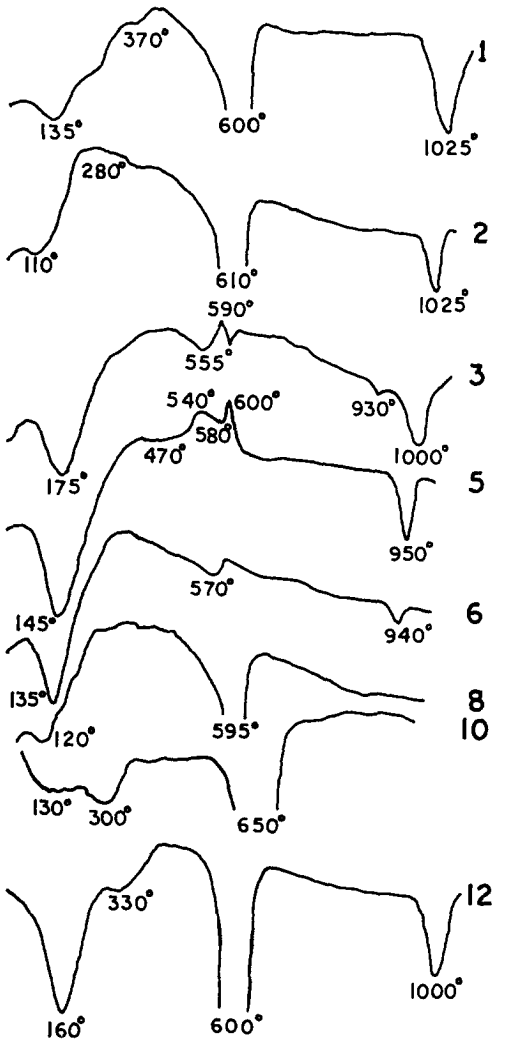

FIG. 5. Differential thermal analysis curves for MnO_2 samples. Numbers at right-hand side denote the catalyst sample numbers.

characterized by a sharp change in weight loss in the TGA curve. In samples 3 and 5 the endothermic peak is immediately followed by a small exothermic effect indicating the recrystallization of poorly crystalline reduced oxides. (iv) Endothermic decomposition of Mn_2O_3 to Mn_3O_4 in the temperature region of 850 to 1050°C. This effect is sometimes poorly defined and lies beyond 1050°C for well-crystallized samples such as β-MnO_2.

The thermograms of two component (MnO_2–CuO) catalysts are essentially similar to those of their precursor MnO_2 except that peaks are smaller due to a smaller amount of manganese dioxide.

The data accumulated from the thermal decomposition characteristics of the samples are given in Table 3 which provides valuable information regarding the catalytic activity of manganese dioxide. Thus Fig. 6a shows the relationship between the DTA peak temperature for initial molecular water loss and the activity toward the oxidation of CO. The percentage conversion increases sharply as the peak temperature increases from 120 to 175°C. An exactly opposite behavior is observed in Fig. 6b where the percentage conversion is plotted against the DTA peak temperature for the decomposition of MnO_2 to Mn_2O_3. The two figures clearly indicate that these two DTA peak temperatures are interrelated, i.e., the dehydration temperature of MnO_2 has a profound effect on the stability of the oxide which in turn is again related to the catalytic activity.

Surface area. Table 2 shows that the specific surface areas of poorly crystalline samples prepared from $KMnO_4$ are higher than those of well-crystalline varieties. However, the catalytic activity of the samples does not seem to be entirely dependent on the specific surface area as one can observe from Tables 1A and 2. Various other factors as described in the preceding paragraphs also play important roles in controlling the catalytic activity.

DISCUSSION

The solid-state chemistry of nonstoichiometric manganese dioxide is complicated because many of the properties are related to the nature of the crystalline modifications (*16*). Even minor structural differences may affect the behavior of the samples significantly. Some of the crystalline modifications of MnO_2 such as the

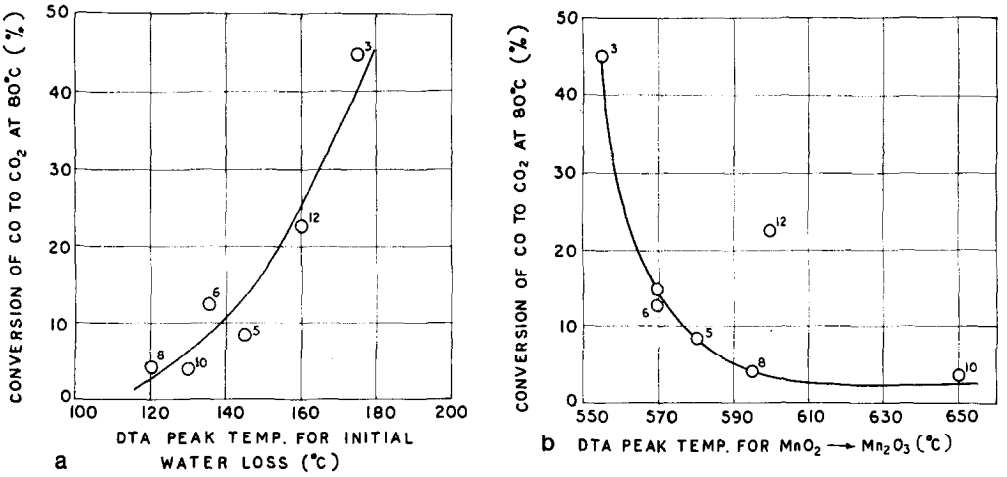

FIG. 6. (a) Relationship between the DTA peak temperature for initial water loss and the conversion of CO to CO_2 over MnO_2 catalyst samples; (b) relationship between the DTA peak temperature for the decomposition of MnO_2 to Mn_2O_3 and the catalytic activity of MnO_2 toward the oxidation of CO. Superscripts denote the catalyst sample numbers.

γ- and δ-variety which are nonequilibrium phases have defect structures and distorted lattices (*17*). However, secondary modifications arising from such imperfections are difficult to identify and are usually a mixture of two or more varieties containing H_2O or OH groups. Glemser *et al.* (*18*) have established the presence of OH groups in the MnO_2 lattice by ir, ESR, and DTA studies. The importance of such compositional OH groups in the battery-active MnO_2 has already been established

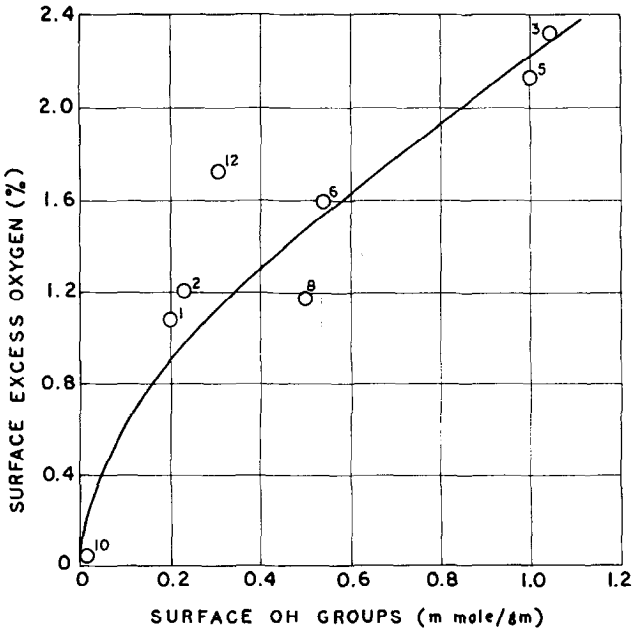

FIG. 7. Correlation between surface OH groups and the surface excess oxygen determined by the KI (pH 7.1) method. Superscripts denote the catalyst sample numbers.

TABLE 3

Thermal Analysis Data of the MnO_2 Catalyst Samples

Sample numbers	Initial loss of physically adsorbed water			Intermediate loss of combined water			Decomposition of MnO_2 to Mn_2O_3			Decomposition of Mn_2O_3 to Mn_3O_4	
	DTA peak temp. (°C) (endo)	DTG peak temp. (°C)	Weight loss at 200°C (%)	DTA peak temp. (°C) (endo/exo)	DTG peak temp. (°C)	Weight loss at 400°C (%)	DTA peak temp. (°C) (endo)	DTG peak temp. (°C)	Weight loss at 700°C (%)	DTA peak temp. (°C) (endo)	DTG peak temp. (°C)
1	135	120	2.21	370 (endo) 420 (exo)	360	4.41	600	600	13.97	1025	1020
2	110	100	2.97	280 (exo)	385	5.15	610	610	14.65	1025	1020
3	175	150	7.50	420 (exo)	—	13.50	555	590	19.75	930	920
5	145	120	10.80	470 (exo)	—	16.71	580	590	20.65	950	940
6	135	120	11.67	335 (exo)	—	16.33	570	570	22.67	940	930
8	120	100	2.75	350 (exo)	—	5.12	595	590	14.76	—	—
10	130	80	0.45	300 (endo)	—	0.68	650	645	10.52	—	—
12	160	150	4.12	330 (endo) 460 (exo)	320	8.12	600	590	17.06	1000	1000

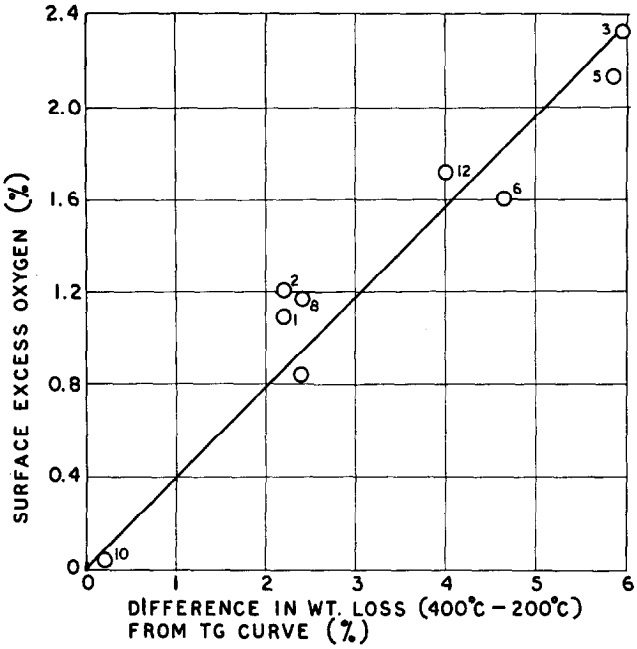

FIG. 8. Correlation between the difference in weight loss at 400 and 200°C (obtained from TGA curves) and the surface excess oxygen determined by KI (pH 7.1) method. Superscripts denote the catalyst sample numbers.

and a detailed bibliography is available in the paper of Tvarusko (*19*). Although various authors (*16*) have proposed different general formulae for nonstoichiometric MnO_2, the one proposed by Brouillet *et al.* (*20*) probably explains the experimental results obtained in the present work. The formula may be written as

$$[MnO_2]_{1-x}[MnOOH]_x$$

or, for electrical neutrality,

$$Mn_{1-x}^{4+}Mn_x^{3+}O_{2-x}^{2-}(OH)_x^-.$$

Since such oxides also contain physically sorbed molecular water a more realistic formula should be

$$Mn_{1-x}^{4+}Mn_x^{3+}O_{2-x}^{2-}(OH)_x^-,\ mH_2O.$$

Lee *et al.* (*21*) observed that certain physisorbed water molecules are bound to the underlying OH groups via hydrogen bonds as has already been found for ThO_2, SiO_2, and Fe_2O_3 [quoted in Ref. (*21*)]. Naturally, the removal of such "structured" water requires a higher desorption energy and hence higher DTA peak temperature. Such energetic desorption leads to lattice distortion and consequent increase in the catalytic activity, as evident from Fig. 6a. Although Brenet (*22*) has stated that both the electrochemical (in dry cell) and the catalytic activity of MnO_2 are dependent on the compositional OH groups, so far no author has shown any experimental evidence. In Figs. 3 and 4 we have shown a definite correlation between the compositional water (or OH groups) and the catalytic activity.

The second stage of water loss in the TG and the DTG curves is primarily a dehydroxylation process. According to Lee *et al.* (*21*) this process consists of two parts; the water from the first part comes from the energetically homogeneous subsurface layer and is dissociatively chemisorbed on the surface. The latter involves the removal of strongly coordinated bulk hydroxyl groups. The dehydroxylation

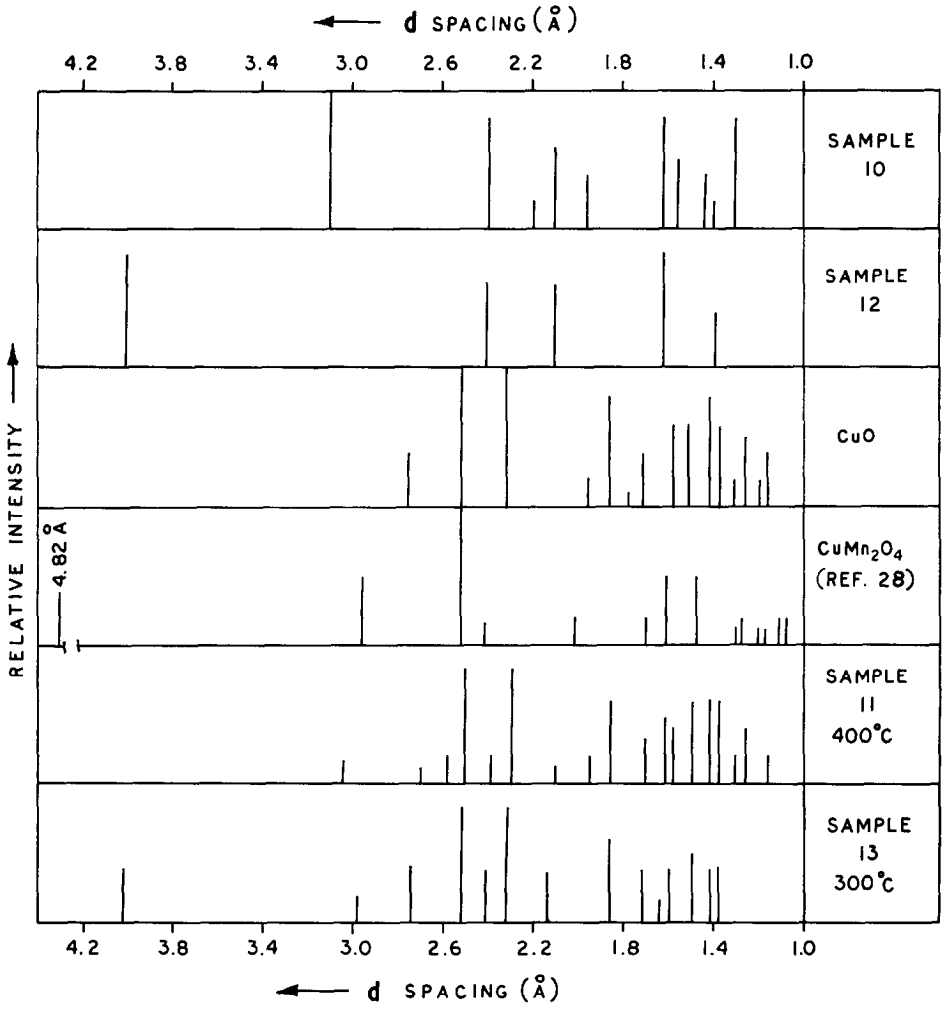

FIG. 9. X-Ray powder pattern of some MnO_2 and MnO_2–CuO catalyst samples.

process within the bulk results in the generation of micropores. The removal of such strongly bound OH groups is also accompanied by the loss of oxygen thereby weakening the lattice structure leading to the decomposition at lower temperature. Therefore, the greater the quantity of compositional water the lower the DTA peak temperature for decomposition to Mn_2O_3 which is thermodynamically a more stable phase.

Though the importance of surface excess oxygen on the catalytic activity of MnO_2 for the oxidation of CO has been repeatedly emphasized by various authors, no satisfactory explanation has so far been forwarded for the origin and nature of this oxygen. However, the general agreement is that during the preparation of the catalyst some oxygen is chemisorbed on the surface which is more mobile and is responsible for the catalytic oxidation of CO even at 20°C. In fact, Brittan *et al.* (*23*) proposed that the primary and rate-controlling step is the adsorption of CO on a site where it can combine with surface oxygen to form an unstable intermediate surface carbonate complex. From the

study of the ir spectra of CO adsorbed on the MnO_2 catalyst Davydov *et al.* (*24*) concluded that the catalyst when treated in a vacuum at 300°C does not oxidize CO even at 200°C. This indicates that the oxidizing properties of MnO_2 are determined by the presence of oxygen dissociatively chemisorbed on the surface. The most firmly bound forms of oxygen are most reactive, but when the catalytic reaction takes place at a low temperature their reaction is blocked by the reaction intermediate (carbonate complex) which is decomposed at 150°C or above. Therefore, oxidation of CO to CO_2 at low temperature takes place with the less firmly bound forms of oxygen.

Brouillet *et al.* (*20*) postulated that during the second stage of water loss oxygen vacancies are created. In an oxidizing atmosphere (e.g., in air) these surface vacant sites chemisorb oxygen. The broadening of the exothermic peak between 250 and 400°C supports this idea, because any oxidation reaction is an exothermic process. The reactions may be written as follows:

$$2\mathrm{MnOOH} \rightarrow \mathrm{MnO_2} + [\mathrm{MnO_2} + (\mathrm{O})\text{vacancy}] + \mathrm{H_2O}$$

$$2[\mathrm{MnO_2} + (\mathrm{O})\text{vacancy}] + \mathrm{O_2} \rightarrow 2\mathrm{MnO_2}.$$

This chemisorbed oxygen has strong oxidizing power and most probably accounts for the surface excess oxygen determined by the KI (pH 7.1) method. The above two equations indicate that there is a correlation between surface OH groups and surface oxygen atoms which has clearly been shown in Fig. 7. This has further been substantiated from Fig. 8 which shows the direct relationship between the difference in weight losses at 400 and 200°C and the surface oxygen content. It can be assumed, as a first approximation, that the type of water present and the mobility of oxygen in the MnO_2 lattice may be closely interrelated to provide a suitable environment for the catalytic reaction to take place.

Since in the foregoing paragraphs it has been proposed that the compositional

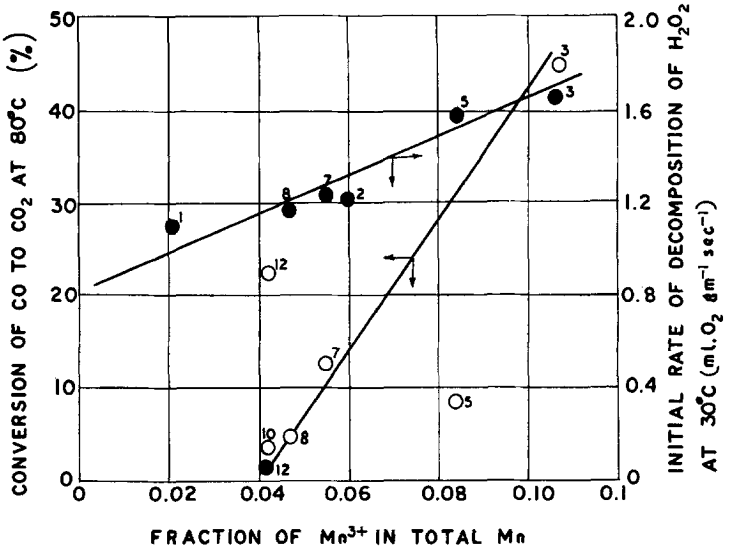

FIG. 10. Relationship between catalytic activity and the Mn^{3+} content of MnO_2 catalysts. Superscripts denote the catalyst sample numbers.

water (or OH groups) in MnO_2 occur mostly as MnOOH, it is expected that the catalytic activity should increase with increase in Mn^{3+} content. This proposition derives some support from Fig. 10 which shows the plot of activity for the oxidation of CO and the decomposition of H_2O_2 vs Mn^{3+} content in the MnO_2 catalyst samples.

It has been observed (*22*) that small metal ions in the MnO_2 lattice may become oxidized or reduced without changing their positions unless the process is sufficient to lead to a new phase. Here perhaps lies the actual reason for the catalytic activity of nonstoichiometric MnO_2, i.e., as in the $CuMn_2O_4$ spinel structure electron exchange between Mn^{4+} and Mn^{3+} can easily take place in the solid phase without the ions changing their positions (*25*). This observation also shows that in contrast to the present belief the presence of some OH groups appears necessary for the activity of MnO_2 toward the oxidation of CO. In other words, completely dehydroxylated (or oxidized) MnO_2 is not an active catalyst for the low-temperature oxidation of CO.

The lattice parameters of MnO_2 catalyst samples as shown in Table 2 indicate that the area of the *ab* plane is much higher than either the *bc* or the *ca* planes. Besides, the apices of the MnO_6 octahedra which are the basic building units in the chain structure of MnO_2 crystals, are protruded on the *ab* plane. Anion vacancies probably occur at the apices thereby rendering the adsorbed ligand accessible to the metal ion. These observations indicate that catalytically active centers are possibly concentrated on the (001) plane. The high activity of Cu_2O for the oxidation of CO has been explained by Stone (*26*) from a similar observation on the unique crystal structure of Cu_2O.

The sharp increase in catalytic activity of two component catalysts (MnO_2–CuO) such as samples 7, 9, and 13 toward the oxidation of CO can also be explained from the presence of MnOOH on the surface of MnO_2. Since $Cu(OH)_2$ was precipitated by adding 1:1 NH_4OH to $Cu(NO_3)_2$ solution in the presence of solid MnO_2 there was no possibility of manganese dissolution in such an alkaline medium. Therefore, the only possibility of bringing Cu^{2+} on the surface of MnO_2 is through ion exchange which is known to occur in hydrated MnO_2. Extensive work (*27*) has been done on this subject:

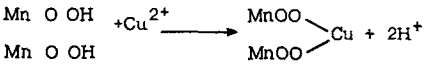

The formation of such "surface $CuMn_2O_4$" will depend upon the exchange capacity of the manganese dioxide. The absence of any promoting effect of CuO in sample 4 is due to the fact that sample 3 was already prepared in the presence of Cu^{2+} ion and the surface was extensively exchanged with Cu^{2+} ions. The increase in catalytic activity with sample 11 is also due to the formation of $CuMn_2O_4$ as is evident from the X-ray diffraction pattern (cf. Fig. 9). The formation of $CuMn_2O_4$ during the simultaneous thermal decomposition of Mn(II) and Cu(II) nitrates has already been reported (*28*). The reason for the poorly developed spinel lines in the powder patterns of samples 11 and 13 is due to the large excess of free CuO in the catalyst samples.

ACKNOWLEDGMENTS

The author wishes to express his sincere gratitude to Prof. Dr. G. M. Schwab for his guidance and valuable advice during the preparation of the manuscript. The author is also thankful to the German Academic Exchange Service (DAAD) for awarding a scholarship which enabled him to carry out a major part of this work in the Institute of Physical Chemistry, University of Munich, West Germany.

REFERENCES

1. Mooi, J., and Selwood, P. W., *J. Amer. Chem. Soc.* **72**, 4333 (1950), **74**, 1750 (1952).

2. Cimino, A., and Indovina, V., *J. Catal.* **33**, 493 (1974).
3. Katz, M., *in* "Advances in Catalysis" (W. G. Frankenburg, E. K. Rideal, and V. I. Komarewsky, Eds.), Vol. 5, p. 177. Academic Press, New York, 1953.
4. O'Hay, J., *in* "Kirk and Othmer Encyclopedia of Chemical Technology" (H. F. Mark, J. J. McKetta, and D. F. Othmer, Eds.), Vol. 13, p. 19. Interscience Publishers, New York, 1967.
5. Ball, S., Goodwin, T. W., and Morton, R. A., *Biochem. J.* **42**, 516 (1948).
6. Turner, D. L., *J. Amer. Chem. Soc.* **76**, 5175 (1954).
7. Harfeinst, M., Bavley, A., and Lazier, W. A., *J. Org. Chem.* **19**, 1608 (1954).
8. Highet, R. I., and Wildman, W. C., *J. Amer. Chem. Soc.* **77**, 4399 (1955).
9. Pitzer, E. C., and Frazer, J. C. W., *J. Phys. Chem.* **45**, 761 (1941).
10. Brooks, C. S., *J. Catal.* **4**, 435 (1965), **8**, 272 (1967).
11. Uchijima, T., Takahashi, M., and Yoneda, Y., *J. Catal.* **9**, 402 (1967).
12. Laragne, J. J., and Brenet, J., *Bull. Soc. Chim. (France)* **9**, 3499 (1968).
13. Livingstone, R., *in* "Techniques of Organic Chemistry" (S. L. Freiss, E. S. Lewis, and A. Weissberger, Eds.), Vol. III, part I, p. 70. Interscience Publishers, New York, 1961.
14. Kobayashi, M., Matsumoto, H., and Kobayashi, H., *J. Catal.* **21**, 48 (1971), **27**, 100 (1972).
15. Hasegawa, S., Yasuda, K., Mase, T., and Kawaguchi, T., *J. Catal.* **46**, 125 (1977).
16. Malati, M. A., *Chem. Ind. (London)*, 446 (1971).
17. Nye, W. F., Levin, S. B., and Kedesy, H. H., *Proc. Annu. Power Sources Conf.* **13**, 125 (1959).
18. Glemser, O., Gattow, G., and Meisiek, H., *Z. anorg. u. allgem. Chem.* **309**, 1 (1961).
19. Tvarusko, A., *J. Electrochem. Soc.* **111**, 125 (1964).
20. Brouillet, B., Grund, A., and Jolas, F. C., *Compt. Rend. Acad. Sci. (Paris)* **257**, 3166 (1963).
21. Lee, J. A., Newnham, C. E., and Tye, F. L., *J. Colloid Interface Sci.* **42**, 372 (1973); Lee, J. A., Newnham, C. E., Stone, F. S., and Tye, F. L., *J. Colloid Interface Sci.* **45**, 289 (1973).
22. Brenet, J. P., *Chimia* **23**, 444 (1969).
23. Brittan, M. A., Bliss, M. A., and Walker, C. A., *A.I.Ch.E. J.* **16**, 305 (1970).
24. Davydov, A. A., Shchekochikhin, Yu, M., and Keier, N. P., *Kinet. Catal.* (Engl. Transl.) **11**, 1019 (1970).
25. Schwab, G. M., and Kanungo, S. B., *Z. Phys. Chem. (N.F.)* **107**, 109 (1977).
26. Stone, F. S., *in* "Advances in Catalysis" (D. D. Eley, P. W. Selwood, and P. B. Weisz, Eds.), Vol. 13, p. 1. Academic Press, New York, 1962.
27. Fuller, M. J., *Chromatogr. Rev.* **14**, 45 (1971).
28. Sinha, A. P. B., Sanjana, N. R., and Biswas, A. B., *J. Phys. Chem.* **62**, 191 (1958).